



---

## MHD Heat and Mass Transfer on Viscoelastic Fluid Flow through an Infinite Oscillating Porous Plate in the Presence of Hall Current with Constant Heat and Mass Flux

Sonia Nasrin<sup>1</sup>, Md. Rafiqul Islam<sup>2</sup>, Md. Mahmud Alam<sup>1</sup>

<sup>1</sup>Mathematics Discipline, Khulna University, Khulna-9208, Bangladesh

<sup>2</sup>Department of Mathematics, Bangabandhu Sheikh Mujibur Rahman Science and Technology University, Gopalganj, Bangladesh

---

**Abstract** The Unsteady MHD viscoelastic fluid flow through a vertical porous plate with thermal diffusion and Hall current effects in the presence of chemical reaction which retained current density. Under this consideration the governing equations of MHD boundary layer flow are reduced to a coupled non-linear system of partial differential equations and are solved by using parameter perturbation technique. The small viscoelastic parameter is used as a perturbation parameter. The obtained equations are solved analytically and using Matlab (R2010a) and Fortran(4.1), the computed results have been obtained with reference to different flow parameters. Finally, the velocity, temperature and concentration profiles are presented graphically.

**Keywords** Heat transfer, Mass Transfer, Viscoelastic Fluid Flow

---

### Introduction

Magneto Hydrodynamics (MHD) is the branch of magneto fluid dynamics, which deals with the flow of electrically conducting fluid in electric and magnetic field. There are many natural phenomena and engineering problems susceptible to Magneto Hydrodynamics analysis. The field of Magneto Hydrodynamics included only the study of partially ionized gases as well as the other names have been suggested, such as magneto fluid mechanics or magneto aerodynamics, but the original nomenclature has been persisted. Engineers employ MHD principles in the design of heat exchangers, pumps and flow meters, in solving space vehicle propulsion, control and re-entry problem, in designing communication and radar system and in developing confinement schemes for controlled fusion. Viscoelastic fluid flow has been generated in the area of heat and mass transfer of the boundary layer along an oscillating porous plate in presence of thermal diffusion in various fields like polymer processing industry in particular in manufacturing process of artificial film and artificial fibers and in some applications of dilute polymer solution in recent years. The boundary layer flow of non-Newtonian fluid in the presence of magnetic field has wide range of application in nuclear engineering and industries. The major significance of the geometry of a textile structure in contributing to resistance to water penetration can be stated in the following manner. Visco-elastic properties can enhance or depress heat transfer rates, depending upon the kinematic characteristic of the flow field under consideration and the direction of heat transfer.

Heat Transfer in MHD Visco-elastic Fluid Flow over a Stretching Sheet with Variable Thermal Conductivity, Non-Uniform Heat Source and Radiation has been investigated by Abel and Mahesha [1]. The visco-elasticity on the flow and heat transfer in a porous medium over a stretching sheet have been discussed by Abel and Veena [2]. MHD free convection and mass transfer flow with Hall current, viscous dissipation, joule heating and thermal diffusion studied by Ajay Kumar Singh [3]. A great deal of work has been carried out to find the analytic solution of visco-elastic fluid flow of non-Newtonian flows over impervious stretching boundary has



been analyzed by Chamkha and Ahmed [4]. The steady mixed convection boundary layer flow due to the combined effect of heat and mass transfer over a stretched vertical surface in a porous medium filled with a viscoelastic fluid under Soret effect in the presence of magnetic field has been investigated by Gbadeyan *et al.* [5]. Viscous dissipative heat on the two-dimensional unsteady free convective flow past an infinite vertical porous plate when the temperature oscillates in time and there is constant suction at the plate has been analyzed by Rajesh and Varma [6]. MHD Free Convection Visco-Elastic Fluid Flow Bounded by an Infinite Inclined Porous Plate in the Presence of Heat Source is studied by Umamaheswar *et al* [7].

Hence our aim is to study MHD heat and mass transfer on viscoelastic fluid flow along an oscillating porous plate in the presence of hall current with constant heat and mass flux. MHD boundary layer equations are reduced to a coupled non-linear system of partial differential equations and are solved by using parameter perturbation technique. The obtained equations are solved analytically and the computed results have been calculated with reference to different flow parameter by using Matlab (R2010a) and Fortran(4.1). Finally the velocity, temperature and concentration profiles are presented graphically.

**The Governing Equations**

Consider two dimensional unsteady flow of an incompressible viscoelastic fluid through porous medium with simultaneous heat and mass transfer along an oscillating infinite porous plate with heat source, chemical reaction and thermal diffusion. The *x*-axis is taken along the upward direction of the fluid flow and *y*-axis is normal to it. The velocity components *u*, *v* and *w* are in the direction of *x*, *y* and *z* direction respectively. If the plate is extended to infinite length, then all the physical variables in the problem are function of *y* and *t* alone. Initially the plate and fluid are in at rest and the plate is set to oscillatory motion. Also it is consider that the fluid and the plate is at rest after that the plate is to be moving with a constant velocity  $U_0$  in its own plate instantaneously at time  $t > 0$ , the species temperature of the plate is raised to  $T_w (> T_\infty)$ , where  $T_w$  is species temperature at the wall of the plate and  $T_\infty$  be the temperature of species far away from the plate. The physical model of the problem is shown in the following figure.

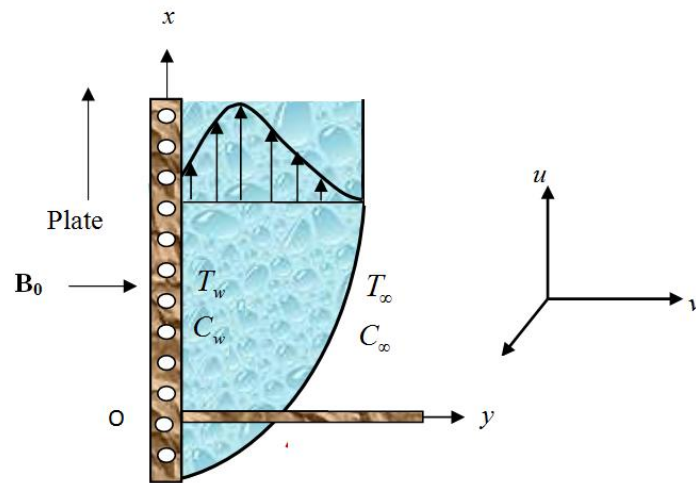


Figure 1: Physical Configuration and Coordinate system

Thus accordance with the above assumptions the basic equations relevant to the problem are as follows:

$$\frac{\partial u}{\partial t} - v_0 \frac{\partial u}{\partial y} = g\beta(T - T_\infty) + g\beta^*(C - C_\infty) - \frac{\nu}{\kappa} u - \frac{1}{\rho} \sigma B_0^2 \frac{(u + mw)}{1 + m^2} + \nu \frac{\partial^2 u}{\partial y^2} - \frac{\kappa_0}{\rho} \left[ \frac{\partial^2}{\partial y^2} \left( \frac{\partial u}{\partial t} \right) - \frac{\partial^2}{\partial y^2} \left( v_0 \frac{\partial u}{\partial y} \right) \right] \tag{1}$$

$$\frac{\partial w}{\partial t} - \nu_0 \frac{\partial w}{\partial y} = -\frac{\nu}{\kappa} w + \frac{1}{\rho} \sigma B_0^2 \frac{(um - w)}{(1 + m^2)} + \nu \frac{\partial^2 w}{\partial y^2} - \frac{\kappa_0}{\rho} \left[ \frac{\partial^2}{\partial y^2} \left( \frac{\partial w}{\partial t} \right) - \frac{\partial^2}{\partial y^2} \left( \nu_0 \frac{\partial w}{\partial y} \right) \right] \tag{2}$$

$$\frac{\partial T}{\partial t} - \nu_0 \frac{\partial T}{\partial y} = \alpha \frac{\partial^2 T}{\partial y^2} - S(T - T_\infty) \tag{3}$$

$$\frac{\partial C}{\partial t} - \nu_0 \frac{\partial C}{\partial y} = D \frac{\partial^2 C}{\partial y^2} + D_T \frac{\partial^2 T}{\partial y^2} - K_1(C - C_\infty) \tag{4}$$

The corresponding boundary conditions for the problem are as follows:

$$u = U_0 \cos \omega t + L_1 \frac{\partial u}{\partial y}, \quad w = U_0 \sin \omega t + L_1 \frac{\partial w}{\partial y}, \quad T = T_w, \quad C = C_w \quad \text{at } y = 0$$

$$u = 0, \quad w = 0, \quad T \rightarrow T_\infty, \quad C \rightarrow C_\infty \quad \text{at } y \rightarrow \infty$$

where,  $u, w$  are the velocity components of the fluid,  $\nu$  is the kinematic viscosity,  $g$  is the acceleration due to the gravity,  $\rho$  is the density,  $\kappa$  is the permeability of the porous medium,  $B_0$  is the constant magnetic field vector perpendicular to the plate,  $\beta$  is the coefficient of thermal expansion,  $\beta^*$  is the coefficient of concentration expansion,  $m = \sigma \beta B_0$  is the Hall parameter,  $\sigma$  is the conductivity of the medium,  $D$  is the diffusivity,  $D_T$  is the coefficient of thermal diffusivity,  $S$  is the heat source parameter and the other symbols have their usual meaning.

**Mathematical Formulation**

The following non-dimensional variables are introduced to obtain the non-dimensional governing equations:

$$u^* = \frac{u}{U_0}, w^* = \frac{w}{U_0}, y^* = \frac{yU_0}{\nu}, t^* = \frac{tU_0^2}{\nu}, \theta = \frac{T - T_\infty}{T_w - T_\infty}, \Phi = \frac{C - C_\infty}{C_w - C_\infty}$$

The following non-dimensional governing equations (dropping the asterisk sign) are obtained as follows:

$$\frac{\partial q}{\partial t} - V_0 \frac{\partial q}{\partial y} = \frac{\partial^2 q}{\partial y^2} + G_r \theta + G_m \Phi - R_c \left( \left[ \frac{\partial^3 q}{\partial y^2 \partial t} - V_0 \frac{\partial^3 q}{\partial y^3} \right] \right) - \frac{1}{K'} q + \frac{M^2}{(1 + m^2)} (-q + im q) \tag{5}$$

$$P_r \frac{\partial \theta}{\partial t} - V_0 P_r \frac{\partial \theta}{\partial y} = \frac{\partial^2 \theta}{\partial y^2} - P_r S' \theta \tag{6}$$

$$S_c \frac{\partial \Phi}{\partial t} - V_0 S_c \frac{\partial \Phi}{\partial y} = \frac{\partial^2 \Phi}{\partial y^2} + S_0 S_c \frac{\partial^2 \theta}{\partial y^2} - K_c S_c \Phi \tag{7}$$

corresponding boundary conditions are as follows:

$$q = e^{i\omega t} + L_1 \frac{U_0}{\nu} \frac{\partial q}{\partial y}, \quad T = T_w, \quad C = C_w \quad \text{at } y = 0$$

$$q = 0, \quad T \rightarrow T_\infty, \quad C \rightarrow C_\infty \quad \text{at } y \rightarrow \infty$$

where  $q = u + iw$  is the non dimensional velocity,  $G_r = \frac{\nu}{U_0^3} g \beta (T_w - T_\infty)$  is the Grashof number,

$G_m = \frac{\nu}{U_0^3} g \beta^* (C_w - C_\infty)$  is the mass Grashof number,  $K' = \frac{\kappa U_0^2}{\nu^2}$  is the Permeability parameter,

$M^2 = \frac{\sigma B_0^2 \nu}{\rho U_0^2}$  is the Heartsman number,  $R_c = \frac{\kappa_0 U_0^2}{\rho \nu^2}$  is the elastic parameter,  $S_c = \frac{\nu}{D}$  is the Schmidt number,  $K_c = K_1 \frac{\nu}{U_0^2}$  is the chemical reaction parameter,  $S_0 = \frac{D_T}{\nu} \frac{(T_w - T_\infty)}{(C_w - C_\infty)}$  is the Soret number,  $V_0 = \frac{\nu_0}{U_0}$  is the suction velocity parameter,  $P_r = \frac{\alpha}{\nu}$  is the Prandtl number, and  $S' = \frac{S\nu}{U_0^2}$  is the heat source parameter.

Due to inadequate boundary condition, a perturbation method has been applied with  $R_c \ll 1$  as a perturbation parameter. This assumption is quite consistent as the model under consideration is valid only for slightly elastic fluid. The following transformation have been considered [7]:

$$q = q_0 + R_c q_1 + O(R_c)^2$$

$$\theta = \theta_0 + R_c \theta_1 + O(R_c)^2$$

$$\Phi = \Phi_0 + R_c \Phi_1 + O(R_c)^2$$

Substituting the value of  $q$ ,  $\theta$  and  $\Phi$  in the above equations, the following equations have been obtained:

**Zereth order equations**

$$\frac{\partial q_0}{\partial t} - V_0 \frac{\partial q_0}{\partial y} = \frac{\partial^2 q_0}{\partial y^2} - \left( \frac{M^2}{(1+m^2)}(1-im) + \frac{1}{K'} \right) q_0 + G_r \theta_0 + G_m \Phi_0 \tag{8}$$

$$P_r \frac{\partial \theta_0}{\partial t} - V_0 P_r \frac{\partial \theta_0}{\partial y} = \frac{\partial^2 \theta_0}{\partial y^2} - P_r S' \theta_0 \tag{9}$$

$$S_c \frac{\partial \Phi_0}{\partial t} - V_0 S_c \frac{\partial \Phi_0}{\partial y} = \frac{\partial^2 \Phi_0}{\partial y^2} + S_0 S_c \frac{\partial^2 \theta_0}{\partial y^2} - K_c S_c \Phi_0 \tag{10}$$

**1<sup>st</sup> order equations**

$$\frac{\partial q_1}{\partial t} - V_0 \frac{\partial q_1}{\partial y} = \frac{\partial^2 q_1}{\partial y^2} - \left( \frac{M^2}{(1+m^2)}(1-im) + \frac{1}{K'} \right) q_1 + G_r \theta_1 + G_m \Phi_1 - \left( \frac{\partial^3 q_0}{\partial y^2 \partial t} - V_0 \frac{\partial^3 q_0}{\partial y^3} \right) \tag{11}$$

$$P_r \frac{\partial \theta_1}{\partial t} - V_0 P_r \frac{\partial \theta_1}{\partial y} = \frac{\partial^2 \theta_1}{\partial y^2} - P_r S' \theta_1 \tag{12}$$

$$S_c \frac{\partial \Phi_1}{\partial t} - V_0 S_c \frac{\partial \Phi_1}{\partial y} = \frac{\partial^2 \Phi_1}{\partial y^2} + S_0 S_c \frac{\partial^2 \theta_1}{\partial y^2} - K_c S_c \Phi_1 \tag{13}$$

Corresponding boundary conditions are as follows:

$$\left. \begin{aligned} q_0 = 0, q_1 = 0, \theta_0 = 1, \theta_1 = 0, \Phi_0 = 1 \text{ and } \Phi_1 = 0 \text{ at } y = 0 \\ q_0 = 0, q_1 = 0, \theta_0 = 0, \theta_1 = 0, \Phi_0 = 0 \text{ and } \Phi_1 = 0 \text{ at } y \rightarrow \infty \end{aligned} \right\}$$

In order to reduce the above system of partial differential equations to a system of ordinary differential equation, the following transformations have been used as follows:

$$q_0(y,t) = q_{00}(y) + q_{01}(y)e^{i\alpha t}$$

$$q_1(y,t) = q_{10}(y) + q_{11}(y)e^{i\alpha t}$$

$$\theta_0(y,t) = \theta_{00}(y) + \theta_{01}(y)e^{i\alpha t}$$



$$\Phi_0(y,t) = \Phi_{00}(y) + \Phi_{01}(y)e^{i\omega t}$$

$$\Phi_1(y,t) = \Phi_{10}(y) + \Phi_{11}(y)e^{i\omega t}$$

Substituting these values in the equations (8)-(13), yields

$$q''_{00} + V_0 q'_{00} - \left( \frac{M^2}{(1+m^2)}(1-im) + \frac{1}{K'} \right) q_{00} = -G_r \theta_{00} - G_m \Phi_{00} \tag{14}$$

$$q''_{01} + V_0 q'_{01} - \left( \frac{M^2}{(1+m^2)}(1-im) + \frac{1}{K'} + i\omega \right) q_{01} = -G_r \theta_{01} - G_m \Phi_{01} \tag{15}$$

$$\theta''_{00} + V_0 P_r \theta'_{00} - P_r S' \theta_{00} = 0 \tag{16}$$

$$\theta''_{01} + V_0 P_r \theta'_{01} - P_r \theta_{01} (S' + i\omega) = 0 \tag{17}$$

$$\theta''_{10} + V_0 P_r \theta'_{10} - P_r S' \theta_{10} = 0 \tag{18}$$

$$\theta''_{11} + V_0 P_r \theta'_{11} - P_r \theta_{11} (S' + i\omega) = 0 \tag{19}$$

$$\Phi''_{00} + V_0 S_c \Phi'_{00} - K_c S_c \Phi_{00} = -S_0 S_c \theta''_{00} \tag{20}$$

$$\Phi''_{10} + V_0 S_c \Phi'_{10} - K_c S_c \Phi_{10} = -S_0 S_c \theta''_{10} \tag{21}$$

Corresponding boundary conditions are as follows:

$$\left. \begin{aligned} q_{00} = R \frac{\partial q_{00}}{\partial y}, \quad q_{01} = 1 + R \frac{\partial q_{01}}{\partial y}, \quad q_{10} = R \frac{\partial q_{10}}{\partial y}, \quad q_{11} = R \frac{\partial q_{11}}{\partial y}, \\ \theta_{00} = 1, \quad \theta_{01} = 0, \quad \theta_{10} = 0, \quad \theta_{11} = 0, \quad \Phi_{00} = 1, \quad \Phi_{01} = 0, \quad \Phi_{10} = 0 \text{ and } \Phi_{11} = 0 \end{aligned} \right\} \text{ at } y = 0 \tag{22}$$

$$\left. \begin{aligned} q_{00} = 0, \quad q_{01} = 0, \quad q_{10} = 0, \quad q_{11} = 0, \\ \theta_{00} = 1, \quad \theta_{01} = 0, \quad \theta_{10} = 0, \quad \theta_{11} = 0, \quad \Phi_{00} = 1, \quad \Phi_{01} = 0, \quad \Phi_{10} = 0 \text{ and } \Phi_{11} = 0 \end{aligned} \right\} \text{ at } y \rightarrow \infty \tag{23}$$

The equations (14)-(21) shows that the coupled ordinary linear differential equations, which can be solved easily by analytically. The analytical solutions of these equations yields velocity, temperature and the concentration profiles of the flow field are as follows:

$$q = a_3 e^{-m_2 y} + a_4 e^{-m_2 y} + a_5 e^{-m_{10} y} + a_6 e^{-m_{18} y} + a_7 e^{-m_{20} y} e^{i\omega t} + R_c (a_8 e^{-m_2 y} + a_9 e^{-m_2 y} + a_{10} e^{-m_{10} y} + a_{11} e^{-m_{18} y} + a_{12} e^{-m_{18} y} + a_{15} e^{-m_{20} y} e^{i\omega t})$$

$$\theta = e^{-m_2 y}$$

$$\Phi = a_2 e^{-m_{10} y} + a_1 e^{-m_2 y}$$

### Results and Discussion

To study the physical situation of the problem, we have computed the numerical values of the velocity, temperature and concentration within the boundary layer for different values of the Heat source parameter ( $S'$ ), the Chemical reaction parameter ( $K_c$ ), suction parameter ( $V_0$ ), Hartmann number ( $M$ ), Elastic parameter ( $R_c$ ), Permeability parameter ( $K_p$ ), Hall parameter ( $m$ ), Schmidt number ( $S_c$ ), Rarefaction parameter ( $R$ ), Soret number ( $S_0$ ) with time  $t = 0.314$ . The effects of various parameters are chosen arbitrary.

The displayed figures from Figs.(2)-(13) are shown that the effects of the above mentioned parameters on the velocities profile. Figs.(2), (4), (6), (8), (9), (10), (11), (12) and (13) are plotted by Fortran4.1 code and Figs. (3), (5) and (7) are plotted by Matlab (R2010a) code which showed that the effects of the various parameters on the primary velocity ( $u$ ) and secondary velocity ( $w$ ) profiles. We observed that the figures are in Fortran 4.1 and Matlab codes are identical.



In Fig. 2, we have seen that with the increase of the suction parameter ( $V_0$ ) the primary velocity  $u$  is decreased but the secondary velocity  $w$  is large increased within the interval  $0 < y < 3.4$  (approx.), further it has a minor decreasing effect from  $y > 3.4$ . We observed that the increase in the values of heat source parameter ( $S'$ ) results in a decrease on the velocity components  $u$  and  $w$  which are represented in Fig. 4. In Fig. 6, we observed that with the increase of the chemical reaction parameter ( $K_c$ ), the primary velocity  $u$  is decreased and the secondary velocity  $w$  is increased within the interval  $0 < y < 1.2$  (approx.) and further it has a decreasing effect from  $y > 1.2$ . From Fig.8, we have seen that the velocity components  $u$  and  $w$  are decreased with the increase of the different values of Permeability parameter ( $K_p$ ). The effect of the Hartmann number ( $M$ ) on the velocity field is shown in Fig.9. It is seen that an increase in Hartmann parameter leads to a large decreased in the velocity components  $u$  and  $w$ . Fig.10 showed that the velocity is very small increase with the increased of the elastic parameter ( $R_c$ ). For the variation of the Hall parameter ( $m$ ) the primary velocity and the secondary velocity are decreased which are shown in the Fig.11. We have seen that an increase in Rarefaction parameter ( $R$ ) primary velocity is increased within  $0 < y < 1.7$  (approx.) and secondary velocity is increased within  $0 < y < 2.1$  (approx.) which are shown in the Fig.12. From Fig.13 we see that the velocity components  $u$  and  $v$  are in increased with the increase of the different values Soret number ( $S_0$ ).

The displayed figures from Fig.(14) - (17) are shown that the effects of the suction parameter ( $V_0$ ) and heat source parameters ( $S'$ ) on the temperature profile. Fig.(14) and (16) are made by Fortran4.1 code and Fig.(15) and (17) are made by Matlab code. Here also we observed that the figures are identical in both code.

From the figures in Fig.(14) we have seen that the temperature profiles are decreased for different values of heat source parameter ( $S'$ ). In Fig.(16) leads to a decreasing effects on the temperature with the increase of the Suction parameter ( $V_0$ ).

The concentration profiles are shown in Fig.(18)-(25) for different values of  $S'$ ,  $V_0$ ,  $K_c$  and  $S_0$ . The displayed figures (18), (20), (22) and (24) are done by Fortran 4.1 code and the Fig. (19), (21), (23) and (25) are done by Matlab code, are both identical.

Fig.(18) shows that the concentration is increased with the increase of heat source parameter ( $S'$ ). For the increase different values of suction parameter ( $V_0$ ), the concentration is decreased which are shown in the Fig.(20). In Fig.(22), it is observed that for different values of chemical reaction parameter ( $K_c$ ), the concentration is decreased with the increase of  $K_c$ . Finally it is seen that in Fig.(24), that for the effect of different values of Soret number the concentration is increased.

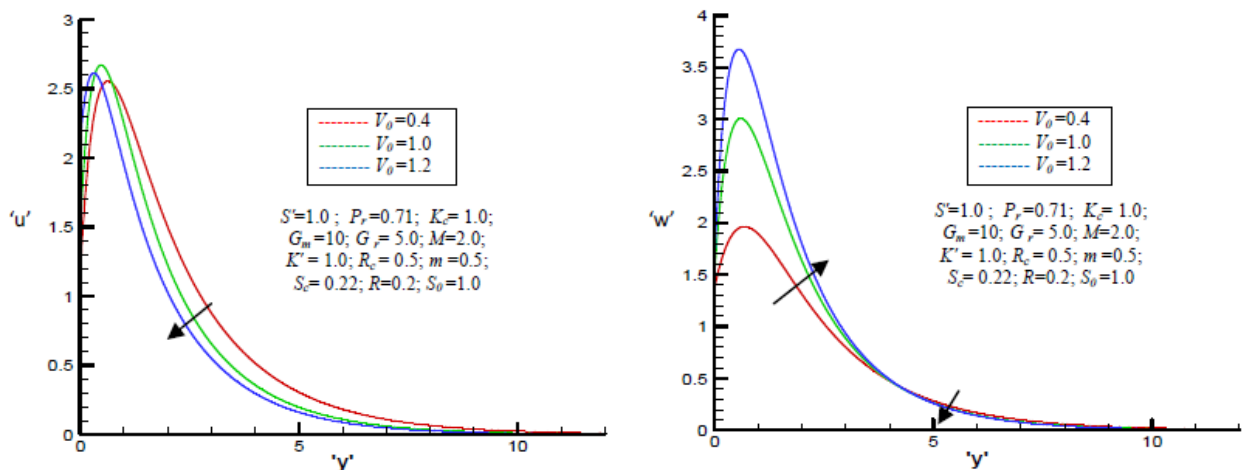


Figure 2: Velocity profiles for different values of suction parameter (using Fortran code)

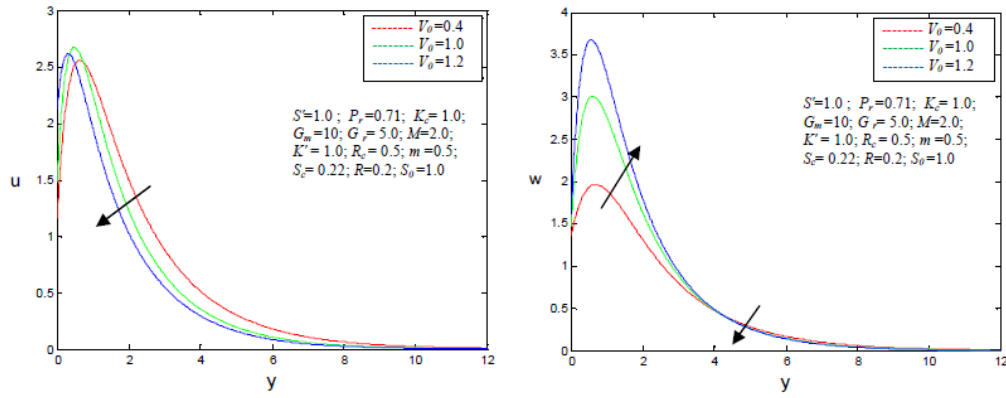


Figure 3: Velocity profiles for different values of Suction parameter (using Matlab code)

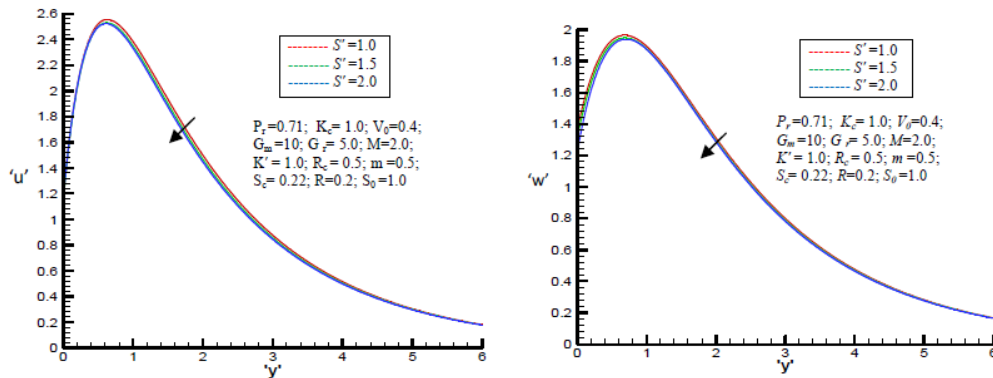


Figure 4: Velocity profiles for different values of heat source parameter (by using Fortran code)

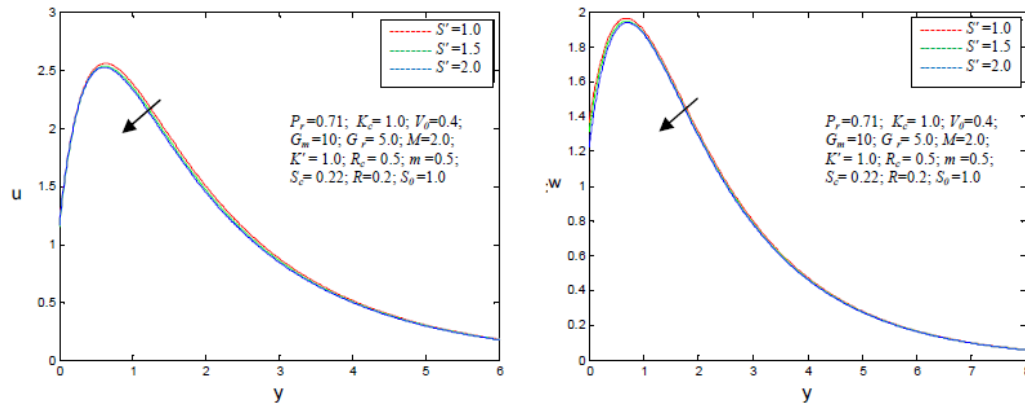


Figure 5: Velocity profiles for difference values of heat source parameter (using Matlab code)

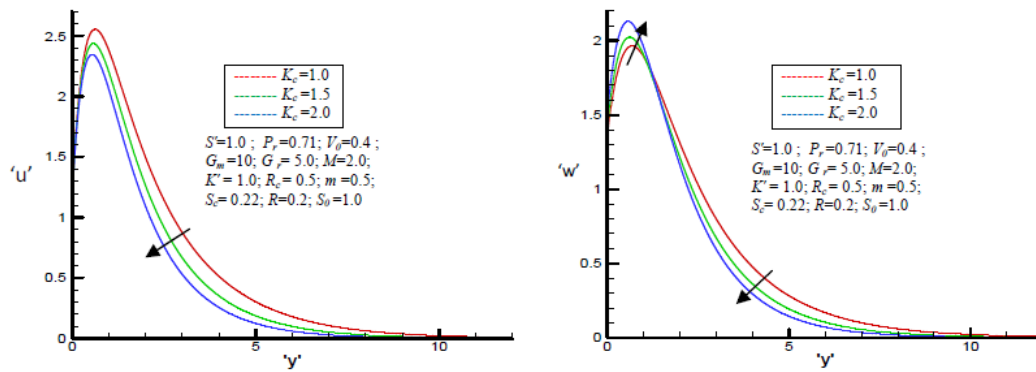


Figure 6: Velocity profiles for different values of chemical reaction parameter (using Fortran code)

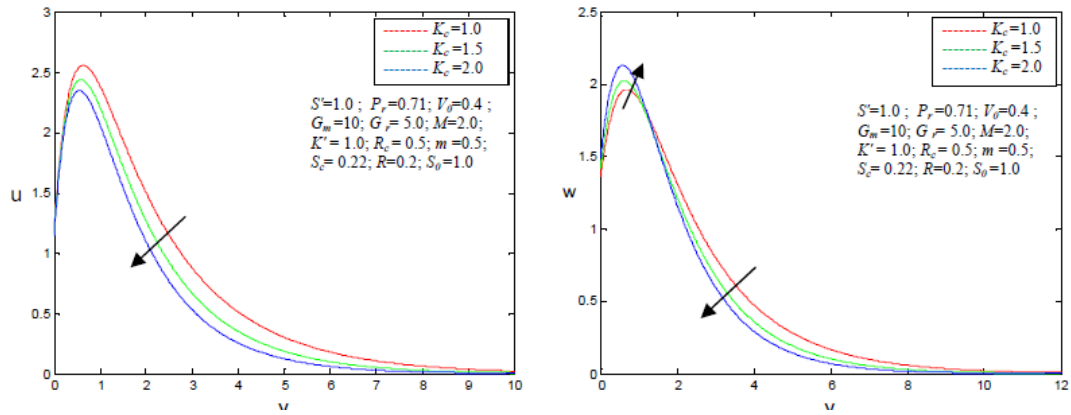


Figure 7: Velocity profiles for different values of chemical reaction parameter (using Matlab code)

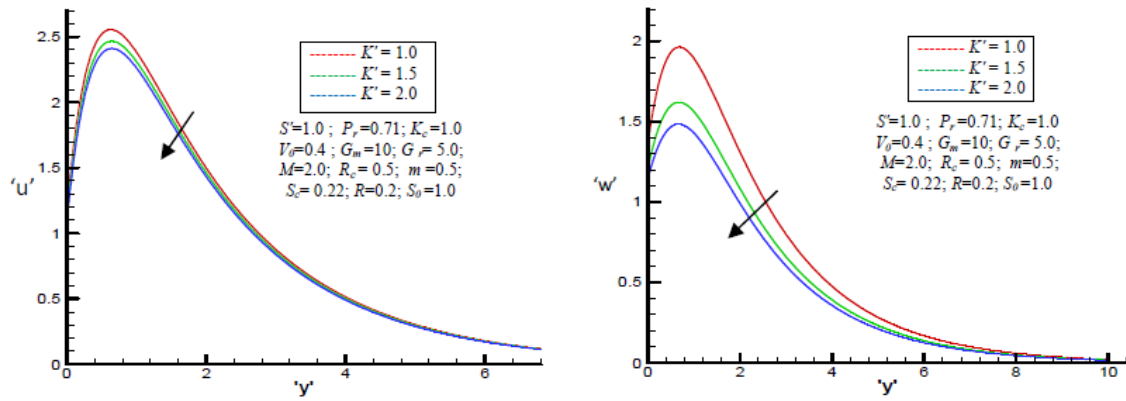


Figure 8: Velocity profiles for different values of Permeability parameter (using Fortran code)

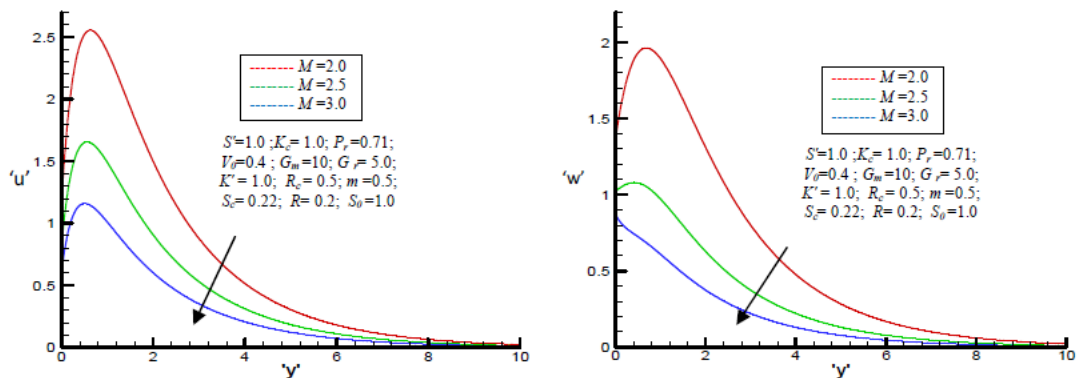


Figure 9: Velocity profiles for different values of Hartmann parameter (using Fortran code)

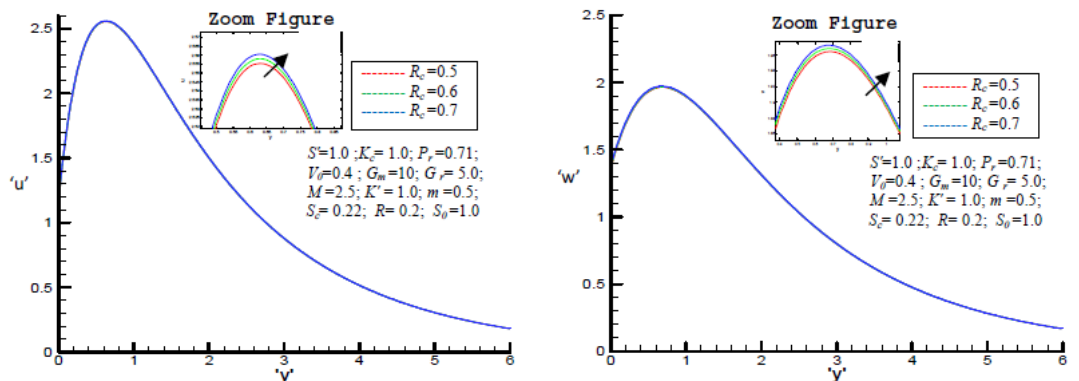


Figure 10: Velocity profiles for different values of Elastic parameter (using Fortarn code)



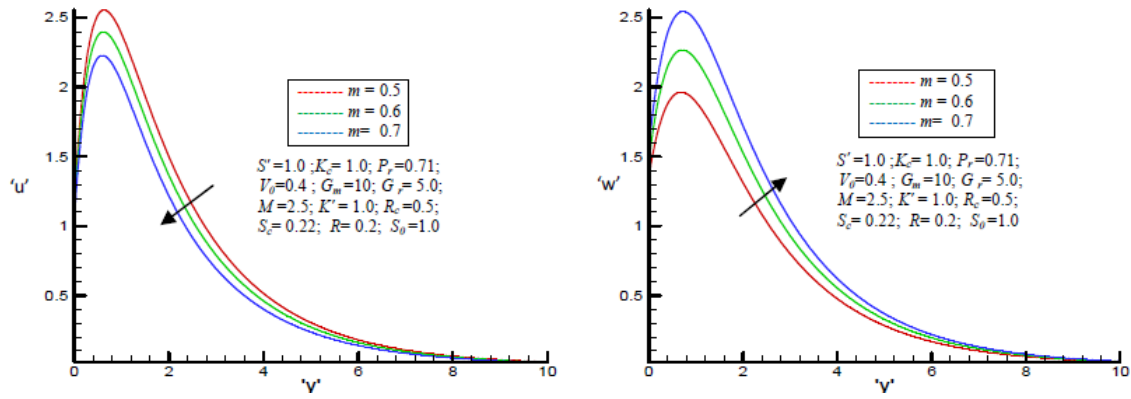


Figure 11: Velocity profiles for different values of Hall parameter (using Fortran code)

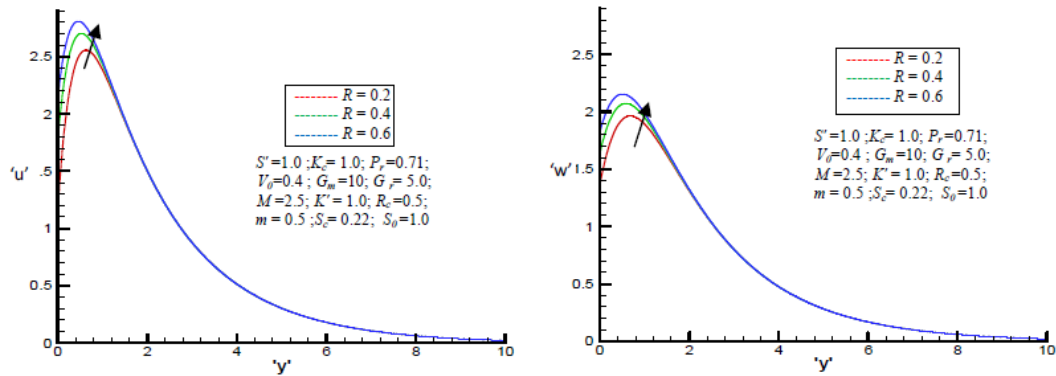


Figure 12: Velocity profiles for different values of Rarefaction parameter (using Fortran code).

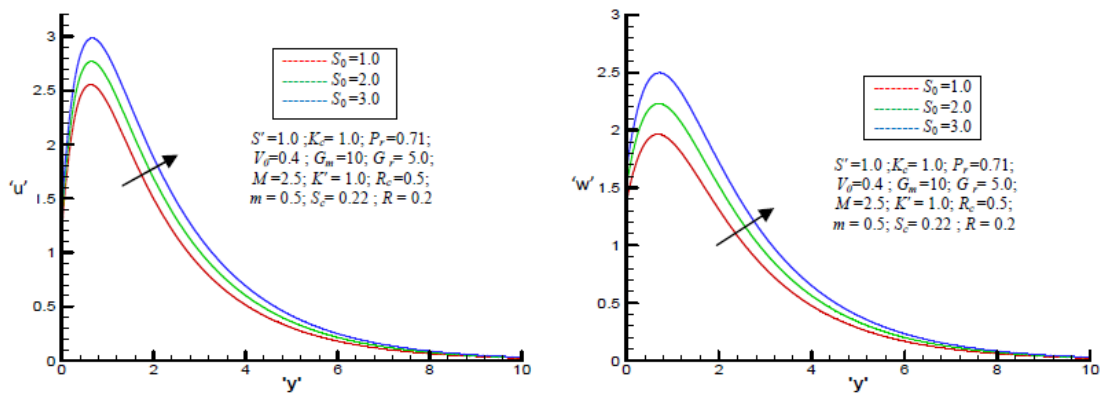


Figure 13: Velocity profiles for different values of Soret number (using Fortran code)

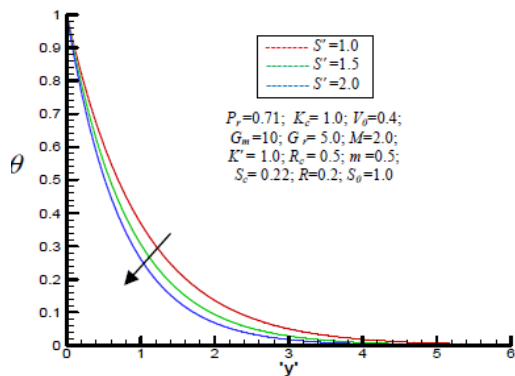


Figure 14: Temperature profiles for different values of heat source parameter (using Fortran code)

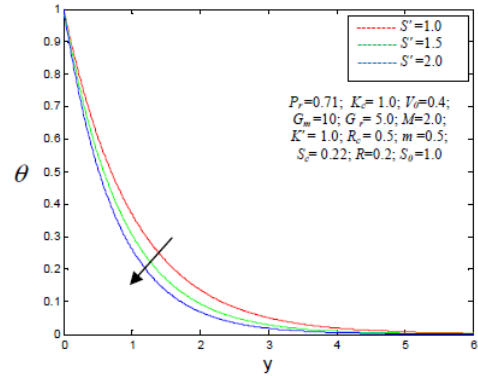


Figure 15: Temperature profiles for different values of heat source parameter (using Matlab code)



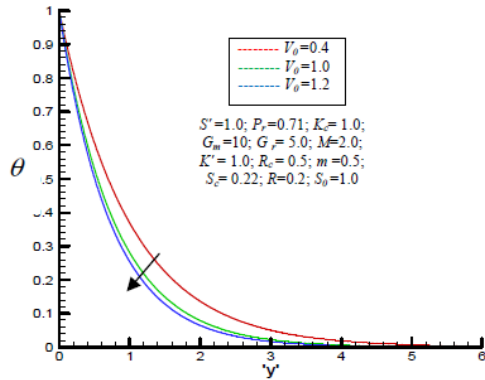


Figure 16: Temperature profiles for different values of t Suction parameter (using Fortran code)

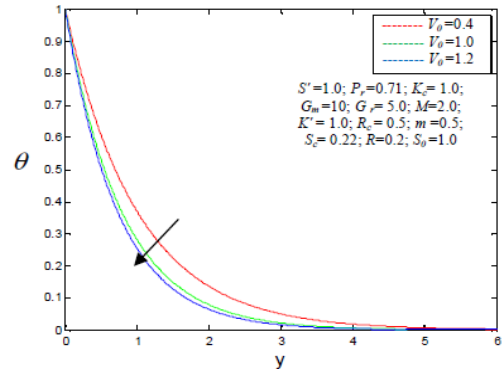


Figure 17: Temperature profiles for different values of Suction parameter (using Matlab code)

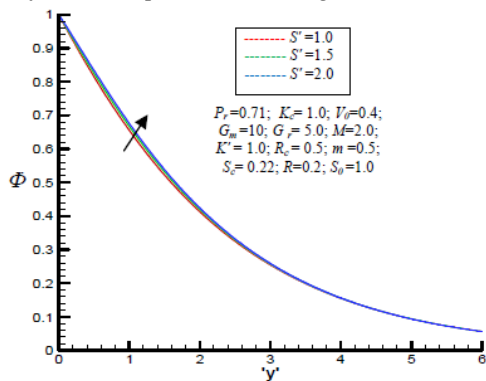


Figure 18: Concentration profiles for different values of heat source parameter (using Fortran code)

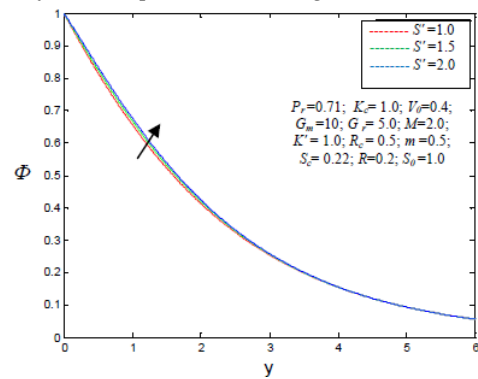


Figure 19: Concentration profiles for different values of heat source parameter (using Matlab code)

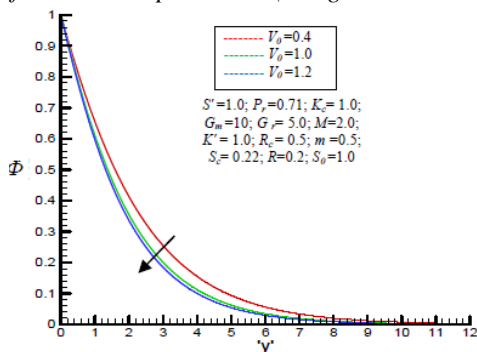


Figure 20: Concentration profiles for different values of Suction parameter (using Fortran code)

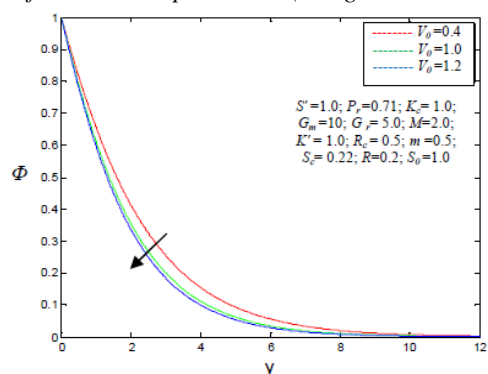


Figure 21: Concentration profiles for different values of Suction parameter (using Matlab code)

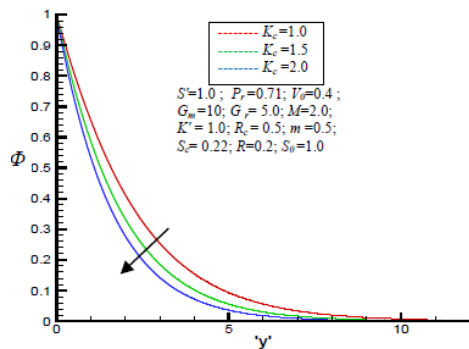


Figure 22: Concentration profiles for different values of chemical reaction parameter (using Fortran code)

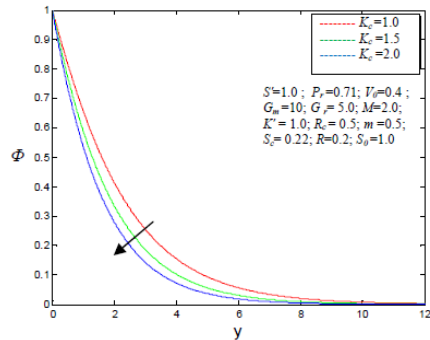


Figure 23: Concentration profiles for different values of chemical reaction parameter (using Matlab code)

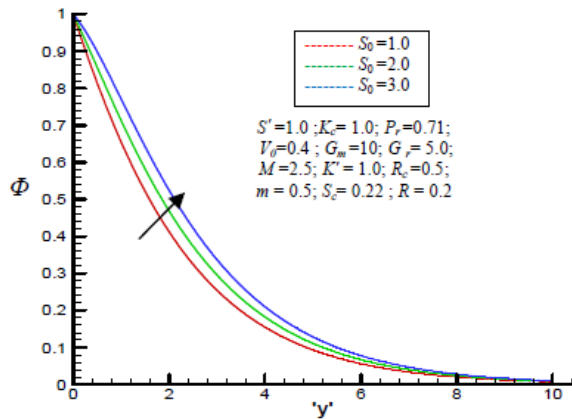


Figure 24: Concentration profiles for different values of Soret number (using Fortran code)

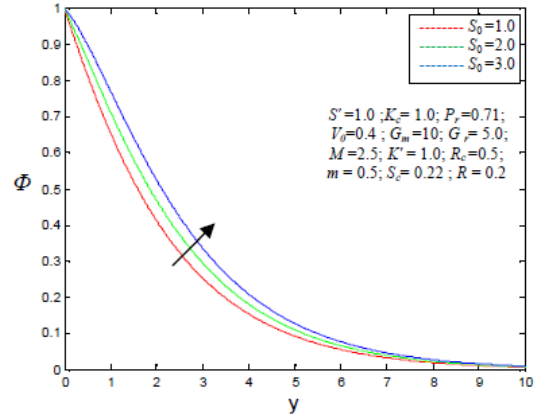


Figure 25: Concentration profiles for different values of Soret number (using Matlab code)

## Conclusion

MHD heat and mass transfer on viscoelastic fluid flow along an infinite oscillating porous plate in the presence of hall current with constant heat and mass flux. The resulting system of dimensionless non-linear coupled partial differential equations is analytically solved by a perturbation method. The effects of different parameters such as Prandtl number, Hartmann number, the elastic parameter, Chemical reaction parameter, Heat source parameter, thermal Grashof number, mass Grashof number, Schmidt number, the suction parameter, Rarefaction parameter and Soret number on velocity, temperature and concentration distribution have been discussed graphically. The resulting figures are identical both Matlab and Fortran computed data.

From the above discussion the conclusion has been drawn as follows:

1. The velocity is decreased with increasing of  $S'$ ,  $M$ ,  $K'$  and  $m$ .
2. The velocity component  $u$  is decreased with increasing of  $K_c$  and  $V_0$ . For the increased of  $K_c$  the secondary velocity  $w$  is increased within the interval  $0 < y < 1.2$  (approx.) and further it has a decreasing effect from  $y > 1.2$ . Also the increased of  $V_0$  the secondary velocity  $v$  is large increased within the interval  $0 < y < 3.4$  (approx.), further it has a minor decreasing effect from  $y > 3.4$ .
3. The velocity is increased with increasing of  $S_0$  and  $R_c$ .
4. The temperature distributions are decreased with increasing of the values of  $S'$  and  $V_0$ . There is no variation of the other parameters.
5. The concentration distributions are decreased with increasing of the, values of  $K_c$  and  $V_0$ . And the concentration distributions are increased with increasing of the values of  $S'$  and  $S_0$ .

## References

- [1]. Abel, S. and Mahesha, N. (2008), "Heat Transfer in MHD Visco-elastic Fluid Flow over a Stretching Sheet with Variable Thermal Conductivity, Non-Uniform Heat Source and Radiation", *Applied Mathematical Modelling*, Vol. 32, pp. 1965-1983.
- [2]. Abel, S. and Veena, P. H. (1998), "Visco-Elastic Fluid Flow and Heat Transfer in Porous Medium over a Stretching Sheet", *International Journal of Non-Linear Mechanics*, Vol. 33, pp. 531-540.
- [3]. Ajay kumar singh (2002), "MHD free convection and mass transfer flow with Hall current, viscous dissipation, joule heating and thermal diffusion" *Indian journal of pure and applied physics*, vol.41, pp-24-35.
- [4]. Chamkha, A. J. and Ahmed, S. E.(2011), "Similarity solution for unsteady MHD flow near a stagnation point of a three dimensional porous body with heat and mass transfer, heat generation/ absorption and chemical reaction", *Journal of Applied Fluid Mechanics*, vol. 4, pp. 87-94.
- [5]. Gbadeyan, J. A., Idowu, A. S., Ogunsola, A. W., Agboola, O. O., Olanrewaju, P. O. (2011), "Heat and mass transfer for Soret and Dufour's effect on mixed convection boundary layer flow over a stretching



vertical surface in a porous medium filled with a visco-elastic fluid in the presence of magnetic field”, *Global Journal of Science Frontier research*, vol. 11(8), pp.96-114.

- [6]. Rajesh and Varma (2011). “Heat and mass transfer effects on MHD flow of an elasto-viscous fluid through a porous medium”, *International Journal of Engineering*, vol.2, pp.205-212.
- [7]. Umamaheswar, M., Verma, S.V.K. and Raju, M.C., (2013), ‘Unsteady MHD Free Convection Visco-Elastic Fluid Flow Bounded by an Infinite Inclined Porous Plate in the Presence of Heat Source, Viscous Dissipation and Ohmic Heating”, *International Journal of Advanced Science and Technology*, vol.61, pp.39-52.

**Appendix**

$$\begin{aligned}
 m_1 &= \frac{-P_r V_0 + \sqrt{P_r^2 V_0^2 + 4P_r S'}}{2}; & m_2 &= \frac{P_r V_0 + \sqrt{P_r^2 V_0^2 + 4P_r S'}}{2}; & m_3 &= \frac{-p_r V_0 + \sqrt{p_r^2 V_0^2 + 4(S' + i\omega)p_r}}{2}; \\
 m_4 &= \frac{p_r V_0 + \sqrt{p_r^2 V_0^2 + 4(S' + i\omega)p_r}}{2}; & m_5 &= \frac{-p_r V_0 + \sqrt{p_r^2 V_0^2 + 4p_r S'}}{2} = m_1; & m_6 &= \frac{p_r V_0 + \sqrt{p_r^2 V_0^2 + 4p_r S'}}{2} = m_2; \\
 m_7 &= \frac{-p_r V_0 + \sqrt{p_r^2 V_0^2 + 4(S' + i\omega)p_r}}{2} = m_3; & m_8 &= \frac{p_r V_0 + \sqrt{p_r^2 V_0^2 + 4(S' + i\omega)p_r}}{2} = m_4; & m_9 &= \frac{-V_0 S_c + \sqrt{V_0^2 S_c^2 + 4K_c S_c}}{2}; \\
 m_{10} &= \frac{V_0 S_c + \sqrt{V_0^2 S_c^2 + 4K_c S_c}}{2}; & m_{11} &= \frac{-V_0 S_c + \sqrt{V_0^2 S_c^2 + 4(i\omega + K_c)S_c}}{2}; & m_{12} &= \frac{V_0 S_c + \sqrt{V_0^2 S_c^2 + 4(i\omega + K_c)S_c}}{2}; \\
 m_{13} &= \frac{-V_0 S_c + \sqrt{V_0^2 S_c^2 + 4K_c S_c}}{2} = m_9; & m_{14} &= \frac{V_0 S_c + \sqrt{V_0^2 S_c^2 + 4K_c S_c}}{2} = m_{10}; & m_{15} &= \frac{-V_0 S_c + \sqrt{V_0^2 S_c^2 + 4(i\omega + K_c)S_c}}{2} = m_{11}; \\
 m_{16} &= \frac{V_0 S_c + \sqrt{V_0^2 S_c^2 + 4(i\omega + K_c)S_c}}{2} = m_{12}; & m_{17} &= \frac{-V_0 + \sqrt{V_0^2 + 4\left[\frac{M^2}{(1+m^2)}(1-im) + \frac{1}{K'}\right]}}{2}; & m_{18} &= \frac{V_0 + \sqrt{V_0^2 + 4\left[\frac{M^2}{(1+m^2)}(1-im) + \frac{1}{K'}\right]}}{2}; \\
 m_{19} &= \frac{-V_0 + \sqrt{V_0^2 + 4\left[\frac{M^2}{(1+m^2)}(1-im) + \frac{1}{K'} + i\omega\right]}}{2}; & m_{20} &= \frac{V_0 + \sqrt{V_0^2 + 4\left[\frac{M^2}{(1+m^2)}(1-im) + \frac{1}{K'} + i\omega\right]}}{2}; \\
 m_{21} &= \frac{-V_0 + \sqrt{V_0^2 + 4\left[\frac{M^2}{(1+m^2)}(1-im) + \frac{1}{K'}\right]}}{2} = m_{17}; & m_{22} &= \frac{V_0 + \sqrt{V_0^2 + 4\left[\frac{M^2}{(1+m^2)}(1-im) + \frac{1}{K'}\right]}}{2} = m_{18}; \\
 m_{23} &= \frac{-V_0 + \sqrt{V_0^2 + 4\left[\frac{M^2}{(1+m^2)}(1-im) + \frac{1}{K'} + i\omega\right]}}{2} = m_{19}; & m_{24} &= \frac{V_0 + \sqrt{V_0^2 + 4\left[\frac{M^2}{(1+m^2)}(1-im) + \frac{1}{K'} + i\omega\right]}}{2} = m_{20}; \\
 m_5 &= m_1; & m_7 &= m_3; & m_{13} &= m_9; & m_{15} &= m_{11}; & m_{17} &= m_{21}; & m_{23} &= m_{19}; \\
 m_6 &= m_2; & m_8 &= m_4; & m_{14} &= m_{10}; & m_{16} &= m_{12}; & m_{18} &= m_{22}; & m_{20} &= m_{24}; \\
 a_1 &= \frac{-S_0 S_c m_2^2}{m_2^2 - V_0 S_c m_2 - K_c S_c}; & a_2 &= 1 - a_1; & a_3 &= \frac{-G_r}{m_2^2 - V_0 m_2 - \left[\frac{M^2}{(1+m^2)}(1-im) + \frac{1}{K'}\right]};
 \end{aligned}$$

$$\begin{aligned}
 a_4 &= \frac{-a_2 G_m}{m_{10}^2 - V_0 m_{10} - \left[ \frac{M^2}{(1+m^2)}(1-im) + \frac{1}{K'} \right]} ; & a_5 &= \frac{-a_1 G_m}{m_2^2 - V_0 m_2 - \left[ \frac{M^2}{(1+m^2)}(1-im) + \frac{1}{K'} \right]} ; \\
 a_6 &= \frac{-1}{(1+Rm_{18}e^{-m_{18}y})} \left\{ (1+Rm_2e^{-m_2y})a_3 + (1+Rm_{10}e^{-m_{10}y})a_4 + (1+Rm_2e^{-m_2y})a_5 \right\} \\
 a_7 &= \frac{1}{(1+Rm_{20}e^{-m_{20}y})} ; & a_8 &= \frac{-V_0 a_3 m_2^3}{m_2^2 - V_0 m_2 - \left[ \frac{M^2}{(1+m^2)}(1-im) + \frac{1}{K'} \right]} ; \\
 a_9 &= \frac{-V_0 a_4 m_{10}^3}{m_{10}^2 - V_0 m_{10} - \left[ \frac{M^2}{(1+m^2)}(1-im) + \frac{1}{K'} \right]} ; & a_{10} &= \frac{-V_0 a_5 m_2^3 + \sqrt{P_r^2 V_0^2 + 4P_r S'}}{m_2^2 - V_0 m_2 - \left[ \frac{M^2}{(1+m^2)}(1-im) + \frac{1}{K'} \right]} ; \\
 a_{11} &= \frac{-V_0 a_6 m_{18}^3}{m_{18}^2 - V_0 m_{18} - \left[ \frac{M^2}{(1+m^2)}(1-im) + \frac{1}{K'} \right]} ; \\
 a_{12} &= \frac{-1}{(1+Rm_{18}e^{-m_{18}y})} \left\{ (1+Rm_2e^{-m_2y})a_8 + (1+m_{10}e^{-m_{10}y})a_9 + (1+m_2e^{-m_2y})a_{10} + (1+Rm_{18}e^{-m_{18}y})a_{11} \right\} ; \\
 a_{13} &= \frac{-V_0 a_7 m_{20}^3 + i\omega a_7 m_{20}^2}{m_{20}^2 - V_0 m_{20} - \left[ \frac{M^2}{(1+m^2)}(1-im) + \frac{1}{K'} + i\omega \right]} ; & a_{14} &= -a_{13} ; & a_{15} &= a_{13} + a_{14} .
 \end{aligned}$$

